

Creep of reaction-bonded silicon nitride

G. GRATHWOHL, F. THÜMMLER

Institut für Werkstoffkunde II der Universität und Institut für Material- und Festkörperforschung, Kernforschungszentrum Karlsruhe, Germany

The high temperature mechanical properties, mainly the creep behaviour of reaction-bonded silicon nitride (RBSN), a new engineering ceramic for the gas turbine, have been a point of considerable interest. During the recent development a remarkable increase of the creep resistance of RBSN has been reached and the latest data show creep rates of below 10^{-6} h^{-1} at 1300° C and 70 to 100 MN m^{-2} . Activation energies between 540 and 700 kJ mol^{-1} and stress exponents of $1 < n \leq 2.3$ have been determined. The viscous flow of a grain boundary phase, controlled by boundary separation, has been considered as the creep rate-controlling step. In this laboratory the internal oxidation during exposure has been found to be a very important factor in determining the creep behaviour of RBSN. An oxide-free RBSN, maintained in this condition during the whole high temperature exposure, appears to be practically creep resistant in a technical sense. The partial conversion of the nitride to oxide phases and the change of chemical composition and microstructure lead to an enhanced creep rate in air compared, for example, with behaviour *in vacuo*. Methods to determine the amount of internal oxidation, namely X-ray diffraction analysis, electron microprobe analysis and Rutherford backscattering of α -particles were used. The deleterious effects of the internal oxidation are explained in terms of the microstructure, mainly porosity and pore size distribution, and ways to avoid this effect are discussed.

1. Introduction

Intensive work has been done in order to develop a new class of ceramics for high performance engineering applications, mainly in gas turbines. Among these, the different types of Si_3N_4 materials play a dominant part. Due to the application temperatures of 1300 to 1350° C , the mechanical and chemical properties at high temperatures are of fundamental importance. For rotating turbine parts an adequate creep resistance must be provided. High creep strains lead not only to an unallowed elongation of the material, but also to uncontrolled stresses in the zone between the strained and unstrained material after cooling down. Although the allowable creep strain in gas turbine components has not been defined exactly, a figure less than 0.5% at 1260° C , $\sim 70 \text{ MN m}^{-2}$ and 200 h was defined for reaction-bonded silicon nitride (RBSN) in gas turbine components [1, 2].

Creep properties have been investigated extensively so far, but very different and in several cases hardly comparable results have been published. Materials of different sources and very different chemical composition and microstructure have been investigated. With respect to the chemical behaviour we must take into account the system: Si_3N_4 -turbine gas is highly unstable thermodynamically. Nevertheless, very creep resistant RBSN qualities have been developed and considerable progress was achieved during recent years.

The aim of this paper is to review some important creep results of RBSN, considering also the work performed in this laboratory. Attention has been drawn to the parameters being important for the creep properties, including the environmental influences.

2. Results

Glenny and Taylor determined the first creep data for Si_3N_4 in 1958 [3, 4]. They investigated several types of RBSN and compared it with HPSN material. They reported the interesting fact the RBSN has better creep resistance at 1200°C than at 1000°C , and the opposite behaviour is true of HPSN. The influence of density and impurity content on creep was emphasized. Parr *et al.* [5, 6], Wells [7] and Thompson and Pratt [8] used different types of material, e.g. with different α/β ratios as well as with additions of SiC. It was claimed that the α -phase is more creep resistant than the β -phase: and that the SiC-containing qualities exhibit the lowest creep rate of the materials investigated. It was stated that the creep rate is probably controlled by a grain boundary mechanism, leading to much higher creep strains than plastic flow within the crystallites. Some of the creep curves shown in all these papers allow more or less clear distinction between a primary and a secondary creep rate; others show a more parabolic behaviour over the total test time. Generally, in this earlier work, very important aspects of creep behaviour and explanations for it have been mentioned, but only few quantitative results for creep dependence on time, temperature, stress, density and structure have been offered.

In the more recent papers kinetic data have been presented and the important technological approach of developing highly creep resistant material was pointed out. The work to be considered here is that of Mangels [9, 10], Restall and Gostelow [11], Washburn and Baumgartner [12], Ud Din and Nicholson [13], Birch *et al.* [14], Lenoë and Quinn [2] and the work of this laboratory [15–21].

2.1. Transient creep

The isothermal strain (ϵ) versus time (t) curves generally exhibit a transient as well as a secondary creep range. The transient range can be very extended (up to 50 h and more) and seems to increase with the applied stress and with increasing porosity of the material. Mainly in the density range of 2.2 to 2.3 or below, high transient creep strains have been observed. Some transient creep curves [15] are shown in Fig. 1.

The most reasonable description of the $\epsilon(t)$ values during transient creep is given by the general parabolic form,

$$\epsilon_t = bt^{1-c} \quad (1)$$

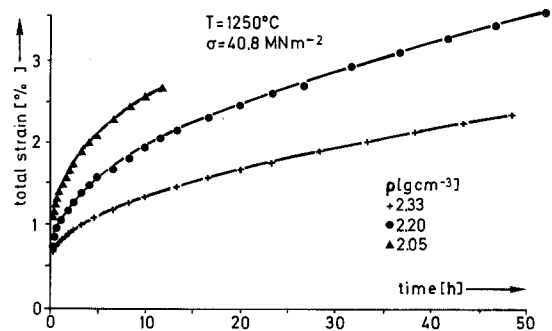


Figure 1 Creep dependence on density of RBSN.

Differentiation leads to the creep rate,

$$\dot{\epsilon}_t = At^{-c} \quad (2)$$

with $A = b(1 - c)$ (A , b and c being constants). Many experimental results on metals as well as on ceramics follow this equation. In RBSN the value of c varies from 0.4 to 0.8 [15]. The initial $\dot{\epsilon}_t$ should be proportional to the steady state creep rate $\dot{\epsilon}_s$ and the total strain in the primary range should be approximately independent of σ and T [22], but this could not be verified generally. This must not be confused with the dependence of $\dot{\epsilon}_t$ on σ . For this a relation

$$\dot{\epsilon}_t \sim e^{B\sigma} \quad (3)$$

has been observed, leading to values for the exponent B between 0.095 and $0.125 \text{ m}^2 \text{ MN}^{-1}$ [15]. Fig. 1 also gives the important influence of bulk density on creep. This effect has been observed by several investigators [3, 5, 8, 15].

A preliminary formula (known from other creep experiments [23])

$$\dot{\epsilon}_p/\dot{\epsilon}_0 = 1 + 0.125 p^2, \quad (4)$$

where $\dot{\epsilon}_p$, $\dot{\epsilon}_0$ = creep rate of the porous and dense material, respectively, and p = porosity (%), can be tried to describe the data obtained in [15], but a physical meaning of this equation is not given. It will be shown below that this porosity influence is not solely a physical effect (e.g. reduction of the effective cross-section), but is chemically based due to the marked influence of pore size and size distribution on internal oxidation and creep. The evaluation of an activation energy is somewhat difficult in this case, and we found values between ~ 500 and 700 kJ mol^{-1} [15]. In order to eliminate structural features, samples with similar strain values have been used for the $\dot{\epsilon}$ versus $1/T$ plots. Lower activation energies have been found at higher stress and lower strain values and vice versa.

There is a statement of principle about the duration of primary creep, derived from the behavior of metals as well as from ceramics: it lasts as long as microstructural processes during creep do not lead to an equilibrium state of the microstructure. Generally hardening, for example by dislocation reactions, is dominant over recovery during primary creep. In the case of Si_3N_4 there is evidence that dislocation motion plays an unimportant role in plastic deformation; the microstructural instability of RBSN is mainly controlled by processes of internal oxidation.

2.2. Steady state creep

The evaluation of the onset of steady state creep ($\dot{\epsilon}_s$) with the secondary (minimum) creep rate $\dot{\epsilon}_s$ is often a matter of discussion, especially in the case of very low creep rates and creep rate changes in relatively short tests. It is also dependent on the strain measurement accuracy. Nevertheless, these figures have been measured in many cases. Generally, the long term tests did not run longer than 200 h and most were concluded before fracture occurred. During secondary creep (where the structural parameters are normally thought of as being unchanged) the equation

$$\dot{\epsilon}_s = A\sigma^n \exp(-Q/RT) \quad (5)$$

is generally fulfilled, where A represents the structural parameters involved (e.g. grain size, porosity), the stress exponent n represents the stress dependence, and temperature dependence is given by the Arrhenius term $\exp(-Q/RT)$, Q being the activation energy of the rate-controlling step. This equation holds in many practical cases for certain ranges of stresses, strains and temperatures.

In Fig. 2 a collection of published results on creep rates of RBSN is presented including our own measurements. The results are presented in the form of steady state creep rates, if there is any measured at all. Otherwise, if the steady state region has not been reached, the minimum creep rate is given. This plot, containing results of recent experiments and also data from earlier materials, thus represents the development of creep resistant materials. A few of the results published so far could not be included in the figure due to the immeasurably small $\dot{\epsilon}_s$ values obtained. In spite of the large uncertainties in the range of extremely low creep rates, values of 10^{-6} to 10^{-7} h^{-1} indicate highly creep resistant materials, especially if they relate to high stresses and temperatures of

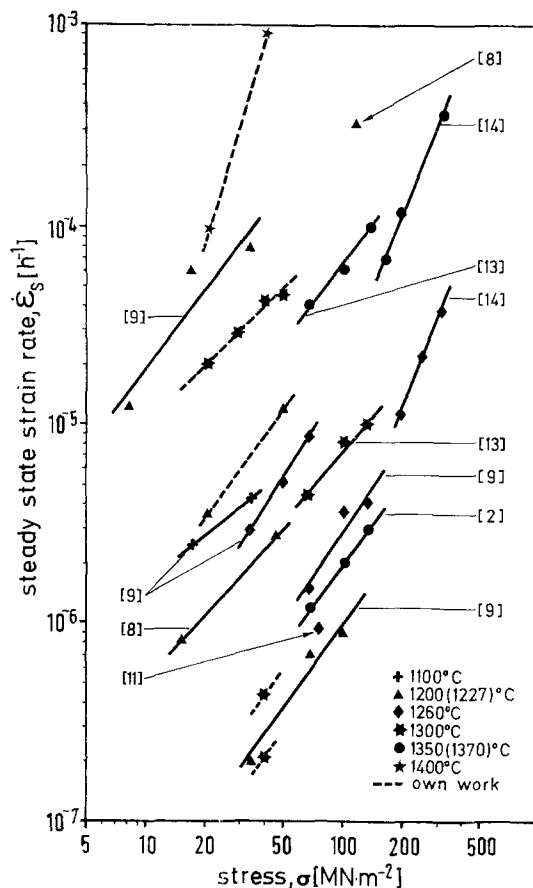


Figure 2 Steady state creep rate of various RBSN materials.

1300°C or above. On the other hand a very wide variety of parameters in fabrication methods (e.g. starting powder, powder preparation, forming procedure, reaction-sintering schedule, atmospheres used) and other variables such as impurities, porosity, pore size and size distribution, and α/β ratio are included in this figure. Thus, under similar test conditions the steady state creep rate can vary by a factor of more than 300.

The results in Fig. 2 have been achieved also with materials made by different forming processes (isostatically pressed, flame sprayed, injection moulded, slip cast) and very different densities (2.1 to 2.69 g cm^{-3}). The influence of H_2 in the N_2 atmosphere during reaction sintering on the creep properties has been described by several authors [9, 10, 13]. The steady state creep rate and the plastic strain after 100 h reach minimal values, if 1 vol.% H_2 is added to the nitriding atmosphere. With this H_2 - N_2 mixture a decrease of the creep rate and the plastic strain by a factor of about 5 is reached in comparison with RBSN material nitrided without H_2 .

It has been also reported, that impurities, mainly Ca, have a deleterious effect on the creep resistance [9, 13]. The few directly comparable results on RBSN show that under similar test conditions the creep rate can be reduced to less than half, if the Ca content comes down from 0.1 to 0.04 wt%. Furthermore, a high α/β ratio is claimed to be favourable for high creep resistance [8, 13], although this was not investigated in detail. An explanation offered for this effect is the higher dislocation density in β -grains compared to α -grains.

According to Equation 5 stress exponents were measured by some investigators [9, 13, 14] and found to be between 1.2 and 2.0 from flexure tests and 2.3 from compression tests. For these measurements and for the evaluation of activation energies, stress change and temperature change experiments, respectively, have been performed with one sample. Additionally, these values have been compared with values received from different samples and excellent agreement has been found. The activation energies range between 500 and 700 kJ mol⁻¹ [9, 13–15].

The creep experiments were performed mostly using the 4-point bending test. Some investigators used the compression test [7, 14], but no correlation between these results and the bending tests has been made. In all cases the equation for elastic behaviour has been taken in order to calculate the stress distribution and the nominal stress.

2.3. Enhanced creep

In most samples investigated so far, no evidence of tertiary creep was observed. This may be, at least partly, a consequence of the relatively short exposure times in these experiments. Also in the case of fracture, tertiary creep was commonly not observed, but the samples failed under the influence of high stresses in the primary creep range [9]. Also, creep fracture at a very high temperature (1450 °C) was found [13]. A few exceptions

where tertiary creep has been observed are reported. These results have been achieved with early materials of a very high porosity [5] and at high temperatures [15].

2.4. Dependence of creep on internal oxidation and microstructural features

According to the actual state of technology, very different qualities of RBSN have been investigated during recent years in this laboratory [15–21]. Some recent results will be presented in the following figures. The samples were fabricated by industrial methods, mainly by the German Annawerk, Rödental-Oeslau. All creep experiments were performed using the 4-point bending test. Table I gives a survey of the origin, the content of some impurities, the α/β ratio, the porosity characteristics and the pre-treatment of a number of different RBSN creep samples.

These samples represent the development of RBSN during recent years. The impurity contents, mainly the important amounts of Ca, differ slightly for the different qualities. A greater difference is seen in the density and the pore sizes. The pore size distributions of the 4 basic materials have been measured by Hg-porosimetry and are illustrated in Fig. 3. Sample 1 is characterized by a rather broad distribution at relatively large pore sizes, whereas the material 2 with the same density as 1 shows much smaller pore sizes. The latest materials (5 and 6) with pore sizes nearly ten times smaller also tend to reduce the volume fraction of the very large pores or voids, and achieve a very narrow distribution of pore sizes.

In Fig. 4 the creep behaviour of these RBSN-qualities is demonstrated. In order to explain the remarkable development of very high creep resistant qualities the difference in impurity contents and α/β ratios can be neglected. The materials 1 and 2 also show nearly the same density, nevertheless, the creep resistance of sample 2 is clearly increased in comparison to sample 1. However,

TABLE I Characterization of RBSN creep samples with respect to Figs. 3, 4 and 6

Specimen	Characterization	Ca (wt %)	Fe (wt %)	Al (wt %)	α/β	Density (g cm ⁻³)	r_{50}^* (μm)	Surface condition
1	Annawerk 98/1	0.11	0.91	0.30	80/20	2.18	0.2	as ground
2	Annawerk 98/2	0.09	0.78	<0.01	90/10	2.14	0.08	as ground
3	Annawerk 98/2	0.09	0.78	<0.01	90/10	2.12	0.08	pre-oxidized
4	Annawerk 98/2	0.09	0.78	<0.01	90/10	2.13	0.08	SiC-coated
5	Annawerk Ar 1200	0.05	0.44	0.30	60/40	2.56	0.035	as ground
6	Norton, NC-350	0.13	0.32	0.38	80/20	2.45	0.034	as ground

* 50% of the pore volume is found below the r_{50} value.

both samples show a large extension of the primary range and a high creep strain as well as a relatively high creep rate. The samples 3 and 4 consist basically of the material 2, but they have been coated before the creep test with SiO_2 (pre-oxidized) and with CVD-SiC, respectively. By this surface sealing treatment the resulting creep behaviour can be markedly changed and the creep deformations and the creep rates have been very

distinctly reduced. The protecting effect of the surface layers against processes which activate the creep processes, i.e. internal oxidation, is obvious.

The fact that internal oxidation of the porous RBSN controls the creep behaviour of poor-quality material has been strengthened by creep experiments in high vacuum. Because of the dissociation of Si_3N_4 , creep strains are very difficult to measure continuously during experiments in vacuum. Therefore the plastic deformation has been determined after the experiment. In Fig. 5 the creep behaviour of a RBSN in air and in vacuum is compared, the creep strain in vacuum being lower than in air by a factor of at least 30.

In order to measure the amount of internal oxidation, an investigation of the samples by X-ray diffraction analysis after the creep experiment has been made. Thereby the amount of crystalline phases along the specimen cross-section has been measured. In Fig. 6 the cristobalite profiles of the samples described in Table I are demonstrated. The poor-quality materials with a high porosity and large pore sizes (1 and 2) are heavily oxidized and show, even in their central parts, an amount of

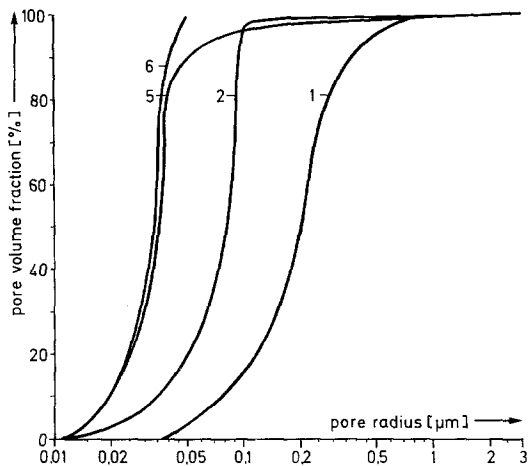


Figure 3 Pore size distributions in RBSN of different qualities.

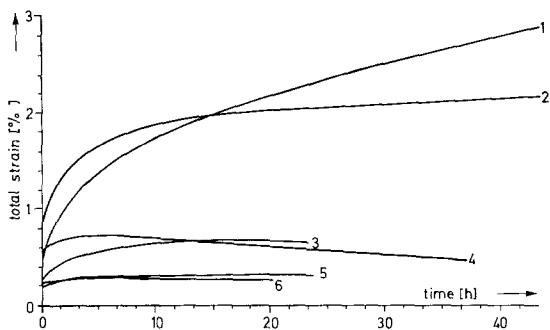


Figure 4 Creep curves for RBSN of different qualities (1300°C , sample 4, 1350°C , 40 MN m^{-2} in air).

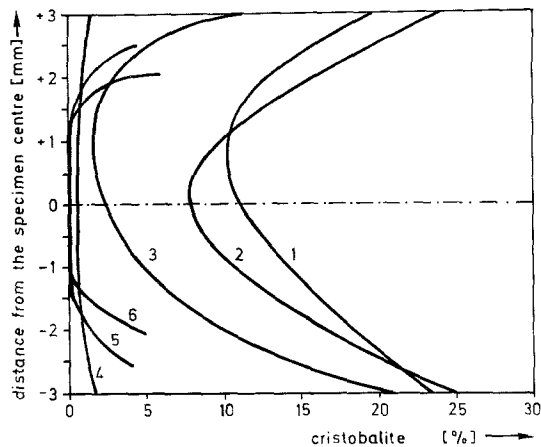


Figure 6 Profiles of cristobalite in RBSN samples after creep experiments.

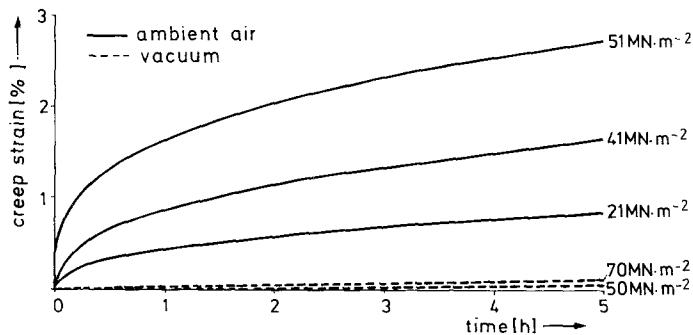


Figure 5 Creep curves for RBSN in vacuum and air at 1300°C .

cristobalite of about 10%. Moreover, in sample 1, an Si_2ON_2 content about as high as the cristobalite value has been found. The same materials, but coated (3 and 4), exhibit much lower amounts of cristobalite, which was expected because of the very strongly increased creep resistance. The sealing effect of the CVD-SiC layer has been proved to be considerably more effective than a simple pre-oxidation.

Obviously, the latest materials (5 and 6) with their high degree of microstructural homogeneity have been shown to be able to protect themselves against considerable internal oxidation. Below a partly oxidized outer layer of the samples, which is about 1 mm thick, practically no cristobalite is found inside the creep samples. These materials show an excellent creep resistance without any special distinction in impurities and α/β ratios over the materials of poorer creep properties. Because the first product of the conversion of Si_3N_4 to SiO_2 is an amorphous silica glass which can crystallize to cristobalite, an unknown amount of amorphous silica may also be present in the creep samples, which could exercise an even stronger influence on the creep behaviour of RBSN than the crystalline phase. Only indirect methods have been used to estimate the amounts of amorphous oxide phases, namely by measuring the total oxygen content and comparing it with the oxygen in the crystalline phases measured by X-ray diffraction analysis. For measuring the oxygen content a nuclear method (Rutherford back-scattering of α -particles) and electron microprobe analysis were used. This part of the work is in progress and some first results by either method show that in addition to the crystalline oxide products a certain amount of amorphous oxide phases can be present [24]. This amount would be dependent primarily on temperature and exposition time. More detailed results shall be presented later.

Another interesting item is the dependence of the creep properties on the thickness of the specimens. Supposing that the oxidation of the porous RBSN beams leads to a "damaged" outer region of the bar, which exhibits a reduced creep resistance a "critical cross-section" of the beams should exist where the "damaged" zones from all surfaces overlap each other in the centre of the specimen. In the materials 1 and 2 the total cross-section of the 6 mm thick specimens is "damaged" and the critical thickness would lie way above the

6 mm cross-section of the sample. The latest materials (5 and 6) very probably show a "damaged" thickness well below 1 mm on each side. In addition, the cristobalite concentration of the oxidized zone in the latest material is considerably lower than in the former. Due to the lack of knowledge about the oxide concentration, necessary for considerable creep enhancement, the really damaged zone in material 5 and 6 could be way below 1 mm and even near zero.

TABLE II Creep strain of RBSN samples of different thicknesses after 20 h at 1300° C, 70 MN m⁻² (preliminary results)

Material	Specimen thickness (mm)	Creep strain after 20 h (%)
2	4	0.89
	2	1.35
5	4	0.12
	2	0.12

In Table II the creep strains of the materials 2 and 5 are compared as measured on creep samples with different cross-sections. A 2 mm thick specimen of material 2 exhibits a nearly 50% higher creep strain compared with the 4 mm thick specimen, whereas no thickness effect has been found so far with the creep-resistant material 5. For the application in gas turbine blades this effect of reduced creep strength of very thin cross-sections (1 mm or less) seems to be important. No creep experiments have been performed so far with samples of such low cross-sections.

3. Discussion

3.1. Influence of microstructure and creep mechanism

The influence of pore size distribution via internal oxidation on creep seems to be an important approach for the explanation of the creep properties of RBSN. Obviously, this oxidation process is in competition with the formation of a protective layer as normally assumed for the high temperature exposure in air. The difficulties of the sealing process of the surface become greater with increasing pore channel diameters. For this sealing mechanism, not the largest but the narrowest parts of a pore channel are responsible. These diameters can be measured exactly by Hg-porosimetry. In spite of the limited number of samples investigated we think a RBSN with pore radii mainly below 0.04 to 0.05 μm behaves favourably in this respect.

Generally, the pore size distribution in a RBSN

depends on the raw material particle size distribution, on the nitriding schedule and on the density of the product. Normally, a RBSN with a higher density should have smaller pores. But the opposite can also occur, at least within certain limits of density, and materials with similar densities can exhibit different pore size distributions.

The oxidation of RBSN occurs in 2 different stages which are controlled by different mechanisms: because the RBSN-qualities investigated so far have a (mainly open) porosity of more than 20%, the oxidation starts with a relatively high reaction rate at the outer and inner surfaces. The gas diffusion into the pores controls this first stage and leads to a distinct oxygen potential gradient from the surface to the centre of the porous material, resulting in a profile of the oxidation products as shown in Fig. 6. The amorphous SiO_2 formed as the first oxidation product has a volume about 80% larger than the Si_3N_4 . In this way the oxidation leads to a reduction of the porosity and of the pore diameters. In order to get a complete closure of the narrow pore necks an oxide layer of a few hundred Ångströms is necessary for the high-quality materials (5 and 6 in Table I). This layer should be formed in air within a few minutes at 1300°C , at least near the surface. On the other hand results have been published [25], where the porosity of RBSN-materials even after 40 h at 1300°C in air is still mainly open. Similar behaviour has been observed with the material 1 (Table I). After a certain time, at which a material with only very small pore diameters is already coated by a dense oxide layer, the inner parts of a specimen with large pores are still accessible and the internal oxidation proceeds very rapidly. At the end of the first stage this material exhibits a large oxidation depth as well as larger amounts of oxide products in the specimen. A model of this process is given in Fig. 7.

The second stage of the RBSN oxidation starts after the formation of the sealing layer and is controlled by the oxygen permeation through the amorphous silica layer or, when the glass crystallizes to cristobalite, by the grain boundary diffusion [26]. In this stage the oxidation rate is very strongly reduced and environmental effects on the creep behaviour may be very much lower than in the first stage. As a consequence, the extent of the internal oxidation depends on the pore size distribution as well as on the temperature.

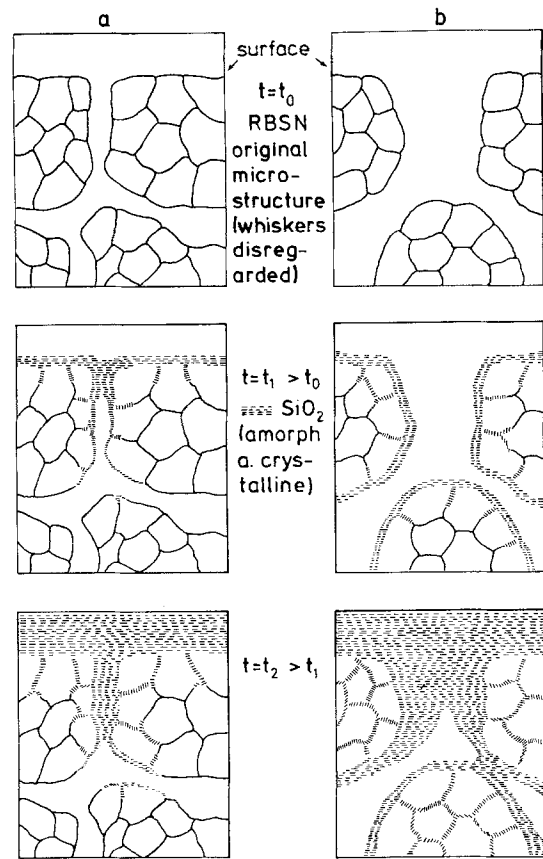


Figure 7 Model of RBSN oxidation. Material with (a) small and (b) large pore sizes.

A large r_{50} value and a broad pore size distribution are unfavourable at any rate.

However, the considerable enhancement of creep due to the oxide products cannot be explained by the assumption that these phases are present only on the pore walls. In this case, no higher creep rates would be expected. Consequently we must assume that during the process of internal oxidation grain boundaries will also be involved (see Fig. 7). This results in destruction of the crystalline nature of the boundaries, at least partly, with the consequence of greater high temperature plasticity.

As a result of these experiments a RBSN with high resistance against internal oxidation and creep should exhibit this very low creep rate in air as well as in vacuum and in protective gases. If the creep rate in vacuum is lower than in air, the material is not of optimum quality. A RBSN without any internal oxide product is fully creep resistant at 1300 to 1350°C in a technical sense.

For further correlation of internal oxidation with creep it is interesting to take the duration of

the primary creep range and the resulting creep rates ($\dot{\epsilon}_t$ and $\dot{\epsilon}_s$) as characterizing features. A material of poor creep resistance due to the internal oxidation exhibits a much longer primary creep range with a high creep rate at the beginning, compared with a creep-resistant material (Fig. 4). In both materials the presence of oxide phases at the grain boundaries which behave viscoelastically can be expected. In the latter material the internal oxidation processes may practically have stopped during the heating or soaking time. Hardly any more oxide products will be formed in the specimen during the creep test and a steady state creep rate may be achieved within a short time. Because of the very limited amount of oxide phases, the creep behaviour of the specimen cannot be controlled by a pure Newtonian viscous process and the stress exponent (n , Equation 5) will be expected to be greater than 1, which has been verified by all published experiments. In such a system the creep rate can be deduced from the relative grain movement which is controlled by the rate at which geometrical obstacles against this displacement can be overcome [27, 28]. The irregular grain boundaries in the extremely fine but unequally formed microstructure of RBSN together with the insufficient oxide layer thickness act as such obstacles.

In materials with large pores and low creep resistance, the internal oxidation has reached a higher level at the end of the soaking time. Thus, a higher creep rate has been found at the beginning of the creep test, which can be related to the higher oxide content, that is, to the increased thickness of the oxide layers. Measurements [29] show that the internal oxidation also proceeds in this material during the creep experiment. An enhanced (tertiary) creep should be the result of this synchronous increase of the oxide content, but a very extended primary creep range has been observed. This behaviour could be due to the crystallization of the amorphous silica to cristobalite, overcompensating the creep-enhanced influence of the preceding internal oxidation. A higher amount of cristobalite in the boundary phase at the expense of amorphous phases leads to a reduction in the creep rate of RBSN by means of higher refractoriness and higher thermal activation for viscous processes in the boundary layer. Nevertheless, the rate-controlling process seems to be the same for materials both with very low and with high internal oxidation. In certain materials

the creep mechanism may be modified to grain boundary sliding with the glide accommodation by cavity formation as described in [30] and claimed for RBSN for example in [14]. This may happen mainly in materials with more regular grains and microstructure and sufficient boundary layer thickness. As a matter of fact, this is very difficult to observe directly in RBSN due to its very fine grain structure. In principle one can understand the co-operation of gliding and cavity formation and growth processes for a limited time, depending on the stress level, but after sufficient boundary sliding and cavitation, cracks will be formed and specimen failure will eventually result.

3.2. Influence of other material parameters

The porosity dependence of internal oxidation and creep requires a rediscussion of the importance of other material parameters. We think the α/β ratio should not have a large effect on creep properties of RBSN, in spite of the larger possibilities of dislocation movement in β - Si_3N_4 . In materials with internal oxide products, the "true plasticity" of the β -phase should be unimportant as in the hot-pressed material [31]. Only the real plastic behaviour of bulk, oxide-free Si_3N_4 by dislocation motion at very high temperatures, e.g. at 1800°C [32], which has not been measured so far, should be influenced by the α/β ratio. A secondary effect of the α/β ratio on creep by the different oxidation behaviour of α - and β - Si_3N_4 cannot be excluded.

It seems somewhat more difficult to evaluate the influence of impurity contents. In HPSN, the Ca content undoubtedly has a marked, unfavourable effect on creep resistance [32]. The same is claimed for RBSN [9, 13], the reason being a lower viscosity of the glass phase at creep temperatures with increasing Ca content. This was deduced from the relevant phase diagrams [33], which exhibit lower liquidus temperatures if phases with high Ca content are involved. The phase $\text{CaO}-2\text{Al}_2\text{O}_3-2\text{SiO}_2$ is described as especially deleterious for creep resistance [9].

On the other hand a RBSN of even lower quality does not creep greatly in vacuum (Fig. 5). Consequently no or insufficient oxide phase is present in such a material during creep, as in a high-quality material. Thus, in the absence of oxide phases (i.e. of internal oxidation) the Ca content does not seem to be so relevant. In this respect it is interesting to note that the high quality and highly creep resistant Norton RBSN (Table I) does not

have the lowest Ca content. We deduce that the creep dependence on the Ca content in RBSN is less important in high quality materials than in products of low density with low oxidation resistance.

3.3. Possible relation of creep to other material properties

There is some evidence, that a RBSN with a low creep rate exhibits also a high resistance to fatigue and delayed fracture, together with a high stress rupture life and other good properties. This seems possible even in the case when the fracture occurs in the absence of considerable creep. Oxidation effects are claimed to be operative during all these processes [20], thus, the resistance against internal, intergranular or stress corrosion, respectively, should influence the creep, fatigue and delayed fracture properties in a similar way. Experimental work on this aspect is needed.

4. Conclusions

Non oxide ceramics, such as RBSN, are thermodynamically unstable in oxidizing environments. In these porous and multiphase materials a very complex system can be operative during high temperature deformation, especially in oxide-containing products. The most important parameters with respect to creep are the microstructure and the atmosphere. The microstructure, which is determined by fabrication as well as by performance conditions, is the key problem to obtain a highly creep-resistant material. It should be emphasized that it is not sufficient to get an "adequate" microstructure before creep; it must be maintained during the whole time of high temperature exposure.

With respect to the total creep deformation after a certain exposure, the RBSN is generally more creep resistant than HPSN but not as resistant as some SiC products. The total outer fibre creep deformation after 100 h at 1300°C at a 70 to 100 MN m⁻² stress level for RBSN is < 0.1 to 0.2%. Products with steady state $\dot{\epsilon}_s$ values in the order of $\leq 10^{-6}$ h⁻¹ can be defined as materials of very high quality. The creep problem of RBSN, in practice, has apparently been solved by the development of the higher qualities of RBSN and meets the requirements mentioned in the first paragraph. Nevertheless, a further improvement of the material would be worthwhile, e.g. with respect to the high temperature performance of the very thin

cross-sections of the turbine blades (less than 1 mm). Their behaviour, together with the influence of burnt fuel components, still has to be understood. Also, the long-time exposure at moderate temperatures (1000 to 1100°C) where the formation of a surface oxide layer occurs very slowly needs further investigating. The same is true for the behaviour under temperature cycling conditions. Generally, a RBSN of high creep resistance due to a controlled microstructure should also exhibit other favourable low and high temperature properties.

Acknowledgements

This work was carried out with the support of the Bundesministerium für Forschung und Technologie, Bundesrepublik Deutschland, which is gratefully acknowledged. The authors would like to thank their colleagues at the institute for helpful discussions, in particular W. Engel and H. Iwanek for creep experiments, F. Porz for X-ray analyses and Mrs E. Martin and Mrs G. Braun for experimental assistance.

References

1. A. F. McLEAN, E. A. FISHER and R. J. BRATTON, "Brittle materials design, high temperature gas turbine", Interim report, 1974, AMMRC-CTR 74-59.
2. E. M. LENOE and G. D. QUINN, "Deformation of ceramic materials", edited by R. C. Bradt and R. E. Tressler (Plenum Press, New York, 1975) p. 399.
3. E. GLENNY and T. A. TAYLOR, *Powder Met.* **12** (1958) 189.
4. *Idem*, *Powder Met.* **8** (1961) 164.
5. N. L. PARR, G. F. MARTIN and E. R. W. MAY, "Special ceramics", edited by P. Popper (Heywood & Co. London, 1960) p. 102.
6. N. L. PARR and E. R. W. MAY, *Proc. Brit. Ceram. Soc.* **7** (1967) 81.
7. W. M. WELLS, "Silicon nitride as a high temperature radome material", Report UCRL-7795 (1964).
8. D. S. THOMPSON and P. L. PRATT, *Proc. Brit. Ceram. Soc.* **6** (1966) 37.
9. J. A. MANGELS, "Ceramics for high-performance applications", edited by J. J. Burke, A. E. Gorum and R. N. Katz (Brook Hill, Chestnut Hill, 1974) p. 195.
10. *Idem*, *J. Amer. Ceram. Soc.* **58** (1975) 354.
11. J. E. RESTALL and C. R. GOSTELOW, *Proc. Brit. Ceram. Soc.* **22** (1973) 89.
12. M. E. WASHBURN and H. R. BAUMGARTNER, "Ceramics for high-performance applications", edited by J. J. Burke, A. E. Gorum and R. N. Katz (Brook Hill, Chestnut Hill, 1974) p. 479.

13. S. U. DIN and P. S. NICHOLSON, *J. Amer. Ceram. Soc.* **58** (1975) 500.
14. J. M. BIRCH, B. WILSHIRE, D. J. R. OWEN and D. SHANTARAM, *J. Mater. Sci.* **11** (1976) 1817.
15. W. ENGEL and F. THÜMMLER, *Ber. Dt. Keram. Ges.* **50** (1973) 204.
16. G. GRATHWOHL and F. THÜMMLER, *ibid* **52** (1975) 268.
17. W. ENGEL, F. PORZ and F. THÜMMLER, *ibid* **52** (1975) 296.
18. F. THÜMMLER, F. PORZ, G. GRATHWOHL and W. ENGEL, "Science of Ceramics", Vol. 8, (British Ceramic Society, Stoke-on-Trent, 1976) p. 133.
19. G. GRATHWOHL, F. PORZ and F. THÜMMLER, *Ber. Dt. Keram. Ges.* **53** (1976) 346.
20. F. THÜMMLER and G. GRATHWOHL, AGARD report No. 651 (1976).
21. G. GRATHWOHL, F. PORZ and F. THÜMMLER, *Amer. Ceram. Soc. Bull* **55** (1976) 819.
22. B. ILSCHNER, "Hochtemperaturplastizität" (Springer-Verlag, Berlin, 1973).
23. D. BRUCKLACHER and W. DIENST, *J. Nuclear Mater.* **42** (1972) 285.
24. J. LOMBAARD, O. MEYER and G. GRATHWOHL, Progress report IAK Teilinstitute Nuklear Festkörperphysik KFK 2357 (1976) 90.
25. B. D. KRUSE, G. WILLMANN and H. HAUSNER, *Ber. Dt. Keram. Ges.* **53** (1976) 349.
26. J. SCHLICHTING and L. J. GAUCKLER, *Powder Met. Int.* **9** (1977) 36.
27. E. OROWAN, *Geophys. J. Roy. Astron. Soc.* **14** (1967) 191.
28. A. G. EVANS and T. G. LANGDON, "Progress in Materials Science", Vol. 21 (Pergamon Press, New York, 1976).
29. G. GRATHWOHL, unpublished work (1977).
30. F. F. LANGE, "Deformation of ceramic materials", edited by R. C. Bradt and R. E. Tressler (Plenum Press, New York, 1975) p. 361.
31. R. KOSSOWSKY, D. G. MILLER and E. S. DIAZ, *J. Mater. Sci.* **10** (1975) 983.
32. *Idem*, "Ceramics for high-performance applications", edited by J. J. Burke, A. E. Gorum and R. N. Katz (Brook Hill, Chestnut Hill 1974) p. 347.
33. F. M. LEVIN, C. R. ROBBINS and H. F. McMURDIE, "Phase Diagrams for Ceramists" (American Ceramic Society, Columbus, Ohio, 1964).

Received 12 July and accepted 7 October 1977.